Direct Detection of Phospholamban and Sarcoplasmic Reticulum Ca-ATPase Interaction in Membranes Using Fluorescence Resonance Energy Transfer[†]

Benjamin Mueller,[‡] Christine B. Karim,[‡] Igor V. Negrashov,[‡] Howard Kutchai,[§] and David D. Thomas*[,‡]

Department of Biochemistry, Molecular Biology and Biophysics, University of Minnesota Medical School, Minneapolis, Minnesota 55455, and Department of Molecular Physiology and Biological Physics, University of Virginia, Charlottesville, Virginia 22908

Received February 5, 2004; Revised Manuscript Received April 15, 2004

ABSTRACT: We used fluorescence resonance energy transfer (FRET) to detect and quantitate the interaction of the sarcoplasmic reticulum Ca-ATPase (SERCA) with phospholamban (PLB) in membranes. PLB inhibits SERCA only at submicromolar Ca. It has been proposed that relief of inhibition at micromolar Ca is due to dissociation of the inhibitory complex. To test this hypothesis, we co-reconstituted donor-labeled SERCA and acceptor-labeled I40A-PLB (superinhibitory, monomeric PLB mutant) in membranes of defined lipid and protein composition, with full retention of Ca-dependent ATPase activity and inhibitory regulation by PLB. FRET from SERCA to PLB was measured as a function of membrane concentrations of PLB and SERCA, and functional activity was measured on the same samples. The data revealed clearly that the stoichiometry of binding is one PLB per SERCA, and that binding is a strict function of the ratio of total PLB to SERCA in the membrane. We conclude that the dissociation constant of PLB binding to SERCA is far less than physiological PLB membrane concentrations. Binding at low Ca (pCa 6.5), where I40A-PLB inhibits SERCA, was virtually identical to that at high Ca (pCa 5.0), where no inhibition was observed. However, the limiting energy transfer at saturating PLB was less at high Ca, indicating a greater donor−acceptor distance. We conclude that (a) the affinity of PLB for SERCA is so great that PLB is essentially a SERCA subunit under physiological conditions and (b) relief of inhibition at micromolar Ca is due to a structural rearrangement within the SERCA−PLB complex, rather than dissociation.

The Ca-ATPase (SERCA)[1] of the sarcoplasmic reticulum (SR) removes Ca ions from the cytoplasm to relax muscle. In cardiac muscle, this enzyme is regulated by phospholamban (PLB) (*1*), which inhibits SERCA at submicromolar Ca^{2+}. This inhibition can be relieved either by elevation of [Ca^{2+}] to the micromolar range or by phosphorylation of PLB by protein kinase A (PKA). This phosphorylation is regulated via β-adrenergic cascades (*2*) and therefore serves as an adrenergic response element of muscle relaxation. The SERCA−PLB calcium-regulatory system has been implicated in cardiovascular disease (*3*−*9*). Recently, the R9C mutation of PLB in humans was directly linked to development of dilated cardiomyopathy (*10*) and progression to failure of the heart in young adults. A human PLB null phenotype (*8*), contrary to that of mice (*11*−*13*), did not protect against development of heart failure, but instead led to disease in young adults as well. PLB continues to attract attention as a possible target for pharmaceutical intervention (*14*). Gene therapy in hamsters, in which a pseudophosphorylated PLB (S16E) was introduced in vivo, was successful in preventing succession to heart failure (*15*). Elucidation of the physical mechanism by which PLB regulates SERCA is needed to evaluate these results and to develop strategies for intervening in human heart disease.

Most insight into the physical interaction of SERCA with PLB has been obtained indirectly, through effects on function. It has often been suggested that decreased inhibition, due to phosphorylation of PLB, micromolar Ca^{2+}, or mutation, is due to dissociation of PLB from SERCA (K_{d2}), in a delicately balanced dynamic binding equilibrium, which also involves oligomeric interactions within PLB (K_{d1}) and

[†] This work was supported by grants to D.D.T. (NIH GM27906) and to C.B.K (AHA 9930083N). B.M. was supported by a predoctoral fellowship from the Lillehei Heart Institute, University of Minnesota Medical School, followed by a predoctoral fellowship from the American Heart Association (Northland Affiliate).

* To whom correspondence should be addressed. E-mail: ddt@umn.edu. Phone: (612) 625 0957. Fax: (612) 624 0632.

[‡] University of Minnesota Medical School.

[§] University of Virginia.

[1] Abbreviations: $C_{12}E_8$, octaethylene glycol monododecyl ether; Ca, divalent calcium ion (Ca^{2+}); Ca-ATPase, Ca^{2+}/Mg^{2+}-dependent adenosine triphosphatase; DABCYL-SE, 4-((4-(dimethylamino)phenyl)azo)-benzoic acid succinimidyl ester; DBU, 1,8-diazobicyclo[5.4.0]undec-7-ene; DIEA, *N*,*N*-diisopropylethylamine; DMF, *N*,*N*-dimethylformamide; DOPC, dioleoylphosphatidylcholine; DOPE, dioleoylphosphatidylethanolamine; EGTA, ethylene glycol bis(β-aminoethyl ether) *N*,*N*,*N*′,*N*′-tetraacetic acid; ErITC, erythrosin isothiocyanate; Fmoc, 9-fluorenylmethyloxycarbonyl; FRET, fluorescence resonance energy transfer; HBTU, 2-(1*H*-benzotriazole-1-yl)-1,1,3,3-tetramethyluronium hexafluorophosphate; HOBt, 1-hydroxybenzotriazole; HPLC, high-performance liquid chromatography; IAEDANS, 5-((((2-iodoacetyl)amino)-ethyl)amino)naphthalene-1-sulfonic acid; IUs, international units; K_d, dissociation constant; MALDI-TOF-MS, matrix-assisted laser desorption/ionization time-of-flight mass spectroscopy; MOPS, 3-(*N*-morpholino)propanesulfonic acid; NADH, nicotinamide adenine dinucleotide (reduced form); pCa, −(log [Ca^{2+}]); PEG−PS, poly(ethylene glycol)−polystyrene (graft support); pK_{Ca}, −[log(K_{Ca})], calcium concentration at half-maximal ATPase activity; PLB, phospholamban; PVDF, poly(vinylidene difluoride); SERCA, sarco(endo)plasmic reticulum Ca-ATPase; SR, sarcoplasmic reticulum; TFA, trifluoroacetic acid; TPA, time-resolved phosphorescence anisotropy; WT, wild-type.

10.1021/bi049732k CCC: $27.50
Published on Web 06/15/2004

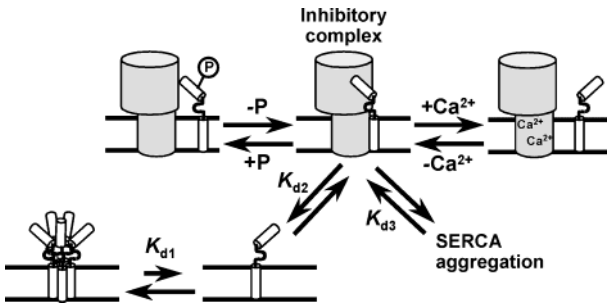

FIGURE 1: Model depicting the role of dynamic protein−protein interactions in the regulation of SERCA by PLB (based on refs *16*−*19*). The present study addresses the proposal that inhibitory interactions between SERCA and PLB are diminished by elevated Ca^{2+}, resulting in a large increase in the dissociation constant K_{d2}.

within SERCA (K_{d3}) (Figure 1; *16*−*20*). To test this hypothesis, it is necessary to measure the dissociation constant (K_{d2}) for the binding of PLB to SERCA directly and quantitatively, and to determine whether changes in K_{d2} correlate with changes in function.

The SERCA enzyme has been shown to co-immunoprecipitate with coexpressed PLB in detergent solution (*21*), with the interaction decreased by micromolar Ca^{2+}, suggesting that Ca induces dissociation of PLB from SERCA. It was reported that the cytoplasmic domain of PLB can be cross-linked to SERCA in cardiac SR and that elevated Ca^{2+} or phosphorylation of PLB decreases cross-linking (*22*). Similarly, cross-linking in an expression system (*23*, *24*) showed that PLB is preferentially cross-linked to SERCA at submicromolar [Ca^{2+}] in the presence of nucleotide. However, another study showed that PLB cross-links to SERCA in cardiac SR even when [Ca^{2+}] is not controlled and is probably saturating the enzyme (*25*). Cross-linking does not measure K_{d2} quantitatively, since this chemical reaction depends on many factors in addition to binding, and since the cross-linking reaction itself perturbs the equilibrium it is meant to measure.

To measure K_{d2} in a membrane, it is necessary to detect a signal in a functional system that relates directly and quantitatively to this specific protein−protein interaction, and to vary the concentrations of components systematically to define the thermodynamic equilibrium. The PLB−SERCA interaction has been detected previously with spectroscopic probes on either the SERCA enzyme or PLB, but not both simultaneously. Effects of PLB on SERCA have been measured by infrared spectroscopy (*26*), and time-resolved phosphorescence anisotropy (TPA) has been used to measure SERCA rotational mobility (*18*, *27*−*29*) and to correlate PLB inhibition of SERCA with aggregation (*30*). Detailed and quantitative analyses of the dissociation equilibria involved in this system (Figure 1) are needed. Therefore, in the present study, we have used fluorescence resonance energy transfer (FRET) to detect directly the interaction of donor-labeled SERCA with acceptor-labeled PLB in membranes. By using a reconstituted system of defined protein and lipid composition, we have controlled the 2-dimensional membrane concentrations of both proteins. We show through biochemical assays on the same samples that this reconstituted system is fully active and biochemically coupled, and displays normal sensitivity to Ca^{2+}, so the spectroscopic results have direct implications for the molecular mechanism of SERCA regulation.

MATERIALS AND METHODS

Reagents. Octaethylene glycol monododecyl ether ($C_{12}E_8$) and Biobeads SM2 were purchased from Calbiochem (San Diego, CA). Dioleoylphosphatidylcholine (DOPC) and dioleoylphosphatidylethanolamine (DOPE) were purchased from Avanti Polar Lipids (Alabaster, AL). The reagents and equipment for SDS−PAGE (4−20% Tris−glycine Criterion precast polyacrylamide gels and Tris−glycine running buffer) and Western blot analysis (except antibody and [I^{125}]protein A) were purchased from Biorad (Richmond, CA). Hybridoma cells expressing anti-PLB antibody 8A3-D5 were obtained originally from Dr. Diana Bigelow, and the antibody was then produced by Covance Research Products, Inc. (Denver, PA). Radioactively labeled [I^{125}]protein A was obtained from PerkinElmer Life and Analytical Sciences (Boston, MA). Spectroscopic dyes were purchased from Molecular Probes (Eugene, OR). All other reagents and those used in the coupled enzyme assay for measuring ATP hydrolysis rates were of the highest purity available and purchased from Sigma (St. Louis, MO).

Peptide Synthesis and Purification of I40A-PLB. Materials, solvents, instrumentation, and general methods of solid-phase peptide synthesis were essentially as described previously (*31*−*33*). In short, the peptide was assembled on Fmoc-Leu-PEG-PS resin (initial load 0.2 mmol/g) by Fmoc chemistry using a PE Biosystems Pioneer peptide synthesis system. All couplings were done in NMP, mediated by HBTU/HOBt/DIEA (4:4:8 (equiv) with respect to peptide−resin). The *N*-terminal amino group was acetylated using acetic anhydride (*34*). First, an Fmoc removal step (with 20% piperidine and 2% DBU in NMP) was carried out on 200 mg of peptide resin followed by treatment with 0.5 M acetic anhydride in 10 mL of DMF for 2 h. Final deprotection was performed by treatment with 2 mL of freshly prepared solution (82.5% TFA, 5% phenol, 5% thioanisole, 2.5% 1,2-ethanedithiol, 5% water) for 6 h at 25 °C (*35*). The acetylated peptide resin was filtered and cleaved. The cleavage mixture was filtered and resin washed with 2 mL of the same solution. Combined filtrates were concentrated under nitrogen gas, and precipitated in 30 mL of diethyl ether at 0 °C. Precipitated peptide was collected by centrifugation, and washed three times with ice-cold diethyl ether. Crude peptide was dissolved in 5 mL of TFA and purified by HPLC on a C-18 column (Vydac, 218TP54) that had been equilibrated with 95% water, 2% acetonitrile, and 3% 2-propanol. The peptide was eluted using a linear gradient to a final solvent composition of 5% water, 38% acetonitrile, and 57% 2-propanol (*36*). Fractions containing peptides were lyophilized to yield 26 mg of I40A-PLB (12% yield based on starting resin).

Labeling of I40A-PLB. Acetylated (*N*-terminus), cleaved, and purified I40A-PLB was labeled with DABCYL-SE on Lys 3. DABCYL was chosen because it lacks fluorescence emission and, therefore, does not interfere with the donor emission signal. A 10 mg sample of acetylated I40A-PLB was dissolved in 100 mM $NaHCO_3$ (pH 9.0) and 0.1% sodium dodecyl sulfate (SDS). A 10-fold molar excess of DABCYL-SE was added from a 100 mM stock solution in DMF, and the sample was incubated for 16 h at 25 °C with shaking. Unreacted DABCYL-SE was removed by HPLC using a diphenyl column (Vydac, 219TP510; 5 μm, 300⇒, 10 × 250 mm). DABCYL-labeled I40A-PLB (DAB−I40A-

PLB) was eluted in a 30 min, 0−100% A to B gradient with a 2.5 mL/min flow rate (buffer A, 95% H_2O, 2% acetonitrile, 3% 2-propanol, and 0.1% trifluoroacetic acid; buffer B, 5% H_2O, 38% acetonitrile, 57% 2-propanol, and 0.1% TFA). The elution time was approximately 22−25 min. Fractions were lyophilized to yield 6.3 mg of DAB−I40A-PLB (63% yield). The dye concentration in labeled samples was determined by direct sample absorbance in methanol ($\epsilon_{453nm} = 32000$ M^{-1} cm^{-1}).

Chemical Analysis of Labeled PLB. Mass spectra were acquired with a Bruker Biflex III matrix-assisted laser desorption/ionization time-of-flight (MALDI-TOF) system equipped with a nitrogen laser (337 nm, 3 ns pulse length) and a microchannel plate detector. Samples were cocrystallized from a stock solution in methanol with the matrix 3,5-dimethoxy-4-hydroxycinnamic acid (sinapinic acid), and data were collected in the linear mode, positive polarity, with an accelerating potential of 19 kV. Each spectrum was an accumulation of 100−400 laser shots. Amino acid analysis was used to confirm peptide composition and concentration. Purified DAB−I40A-PLB was stored in methanol in the dark at −80 °C until it was used for reconstitution and Western blots.

SERCA Purification and Labeling. SERCA was purified from skeletal muscle of New Zealand white rabbits in 0.01% $C_{12}E_8$ by the Reactive-Red method (*37*) and then flash-frozen and stored in liquid nitrogen after addition of 0.5 mg of lipid (sonicated DOPC and DOPE, 4:1 ratio by weight)/mg of protein. The protein concentration was determined by the Lowry method (*38*), using bovine serum albumin as the standard. Prior to labeling, detergent was removed by the same method used in reconstitution (see below). SERCA was labeled with IAEDANS (labeling buffer: 80 mM KCl, 5 mM $MgCl_2$, 1 mM $CaCl_2$, 20 mM MOPS, pH 6.8) at 18.2 μM enzyme and 273 μM dye for 30 min at 25 °C in the dark. Free dye was removed by centrifugation and washing three times (wash buffer: 20 mM sucrose, 100 mM KCl, 20 mM MOPS, pH 7). The dye concentration in labeled samples was determined from absorbance ($\epsilon_{334nm} = 6100$ M^{-1} cm^{-1} (*39*) after treatment with 0.1 N NaOH and 1% SDS. Samples of AEDANS−SERCA were flash-frozen and stored in the dark in liquid nitrogen until they were used for reconstitution, ATPase assays, and FRET measurements.

Reconstitution. AEDANS−SERCA (donor) was co-reconstituted with DAB−I40A-PLB (acceptor), essentially as described (*40*−*42*) but adapted to modify the SERCA membrane concentration (molar ratio, SERCA/1000 lipids) and PLB-to-SERCA ratio (molar ratio, PLB/SERCA). The desired amount of DAB−I40A-PLB in methanol and lipids (DOPC and DOPE at a 4:1 weight ratio in chloroform) were gently mixed and dried over nitrogen gas to create a thin film. Residual solvent was removed under vacuum and desiccant overnight. Lipids and peptide were solubilized in reconstitution buffer (5 mM $MgCl_2$, 0.1 M KCl, 10% glycerol, 20 mM MOPS, pH 7.0) by vortexing thoroughly, followed by mild sonication for 30 s to form unilamellar vesicles. $C_{12}E_8$ (2 mg/mg of lipid) was added. Samples contained 40 μg of purified AEDANS−SERCA and varying amounts of peptide to obtain molar ratios of 0−20 PLBs/SERCA. Reconstitution buffer contained 30 mM MOPS, instead of previously used imidazole, to optimize fluorescence measurements. This substitution did not affect reconstitution results. Detergent was removed over 3 h using Biobeads SM2 (25 mg/mg of $C_{12}E_8$). SERCA ATPase activity and FRET were measured immediately following reconstitution. Samples were then frozen and stored at −20 °C until gel electrophoresis and Western Blot analysis was done.

ATPase Measurements and Data Analysis. ATPase activity was measured using an NADH-linked, enzyme-coupled microtiter plate assay (200 μL/well) as previously described (*32*, *43*). [Ca^{2+}] was controlled by Ca/EGTA buffering by the method of Fabiato and Fabiato (*44*). The assays were detected at 340 nm on a Spectramax Plus microplate spectrophotometer (Molecular Devices) at 25 °C in the presence of ionophore A23187 to dissipate the Ca gradient building up across the membranes due to ATPase activity. The data were plotted (V vs pCa) and fitted by the Hill equation:

$$V = \frac{V_{max}}{1 + 10^{-n(pK_{Ca} - pCa)}} \quad (1)$$

where V is the initial ATPase rate and n is the Hill coefficient. Data were normalized to the maximal rate, V_{max}, which was obtained from the fit, and replotted to determine the shift in pK_{Ca}. We did not use PLB phosphorylation as a means of modifying the SERCA−PLB interaction, because phosphorylation of I40A-PLB has been shown to have little or no effect on its inhibition of SERCA (*43*).

Fluorescence Measurements and Data Analysis. Steady-state fluorescence spectra were obtained in a 5 × 10 mm quartz cuvette with an ISS-K2 fluorescence spectrophotometer (ISS, Champaign, IL) using an argon ion laser (Coherent, Santa Clara, CA) as the source of excitation at 351.1 nm. Each emission spectrum was the average of two scans with a 1 nm step size, and was corrected by subtraction of a corresponding blank using a reconstituted sample containing unlabeled SERCA at the appropriate SERCA membrane concentration and PLB/SERCA ratio. The sample temperature was controlled using a recirculating water bath set to 25 °C. The free calcium concentration, [Ca^{2+}], was controlled by Ca/EGTA buffering, calculated by the method of Fabiato and Fabiato (*44*). Measurements were conducted in low-Ca (pCa 6.5) buffer (50 mM KCl, 5 mM $MgCl_2$, 0.5 mM EGTA, 210 μM $CaCl_2$, 50 mM MOPS, pH 7.0), where the inhibitory effect of PLB was maximal, and high-Ca (pCa 5.0) buffer (same as low-Ca buffer, except 489 μM $CaCl_2$), where the inhibitory effect of PLB was negligible.

The fluorescence resonance energy transfer efficiency (E)-was calculated from the fractional decrease of steady-state emission of the donor (F_D) due to the presence of the acceptor (F_{DA}):

$$E = 1 - \frac{F_{DA}}{F_D} \quad (2)$$

The donor−acceptor distance R in the saturated SERCA−PLB complex was calculated from

$$R = R_0(E^{-1} - 1)^{1/6} \quad (3)$$

where the Förster distance R_o of this dye pair was calculated from

$$R_o = 9780(J\kappa^2 n^{-4}\phi_D)^{1/6} \quad (4)$$

where n is the refractive index of protein in aqueous solution (1.33), κ is the orientation factor (set to 2/3, corresponding to random orientation), and ϕ_D is the donor quantum yield (0.36 for AEDANS (*45*)). J is the normalized spectral overlap integral of donor emission $F_D(\lambda)$ and acceptor excitation ϵ-(λ)

$$J = \frac{\int F_D(\lambda)\,\epsilon(\lambda)\,\lambda^4\,d\lambda}{\int F_D(\lambda)\,d\lambda} \quad (5)$$

and was calculated by numerical integration using a Microcal Origin 7.0 template.

Time-resolved fluorescence decays were detected to obtain more detailed information about FRET. Decays were obtained in the same 5 × 10 mm quartz cuvette and using identical samples on an instrument developed in collaboration with Dakota Technologies, Inc. (Fargo, ND). This instrument uses a solid-state pulsed laser (frequency-tripled Nd:YAG, 355 nm), operating at a rate of 10 kHz, and acquires the entire fluorescence waveform after each laser pulse, at a time resolution of 0.2 ns/data point. The instrument response function was measured with a light-scattering sample (water) in the same cuvette used for sample measurements and was used in data analysis to determine fluorescence lifetimes (*45*). Excited-state lifetimes (τ_i) and mole fractions (x_i) were obtained by fitting the lifetime-dependent fluorescence exponential

$$F(t) = F_o\sum_{i=1}^{n} x_i e^{-t/\tau_i} \quad (6)$$

to decays with peak intensity F_o. The energy transfer efficiency E was calculated as the fractional decrease of the donor lifetime. A direct comparison with steady-state data was made by calculating the fractional decrease in the average lifetime $\langle\tau\rangle = \sum x_i\tau_i$.

Analysis of FRET due to Specific Binding. The SERCA−PLB interaction can be described by the dissociation equilibrium

$$\text{SERCA}-\text{PLB} \leftrightarrow \text{SERCA} + \text{PLB} \quad (7)$$

This assumes that the stoichiometry of the SERCA−PLB complex is 1:1, consistent with previously reported models (*46*−*48*), and observations that the PLB monomer is the inhibitory species (*16*, *17*). It has been established previously that I40A-PLB is monomeric (*17*, *43*). Therefore, the dissociation equilibrium (eq 7) is not complicated by linkage to the monomer−oligomer equilibrium of PLB (K_{d1} in Figure 1). The dissociation constant K_{d2} for this equilibrium is defined as

$$K_{d2} = \frac{[\text{SERCA}][\text{PLB}]}{[\text{SERCA}-\text{PLB}]} \quad (8)$$

and the fraction of SERCA molecules with bound PLB (x_B) is

$$x_B = \frac{[\text{SERCA}-\text{PLB}]}{[\text{SERCA}] + [\text{SERCA}-\text{PLB}]} = \frac{[\text{PLB}]}{K_{d2} + [\text{PLB}]} \quad (9)$$

The binding of PLB to SERCA can be measured by FRET due to specific binding (E_{SB}):

$$E_{SB} = x_B E_{max} \quad (10)$$

where E_{max} is the maximal FRET value that describes the asymptote of the specific binding hyperbola.

We expect high-affinity binding and hence ligand depletion, so that a significant fraction of the proteins added is actually in the SERCA−PLB complex. Therefore, the concentrations of free ligand and free enzyme must be expressed using mass balance as

$$[\text{PLB}] = [\text{PLB}_{tot}] - [\text{PLB}_{bound}] \quad \text{and}$$
$$[\text{SERCA}] = [\text{SERCA}_{tot}] - [\text{SERCA}_{bound}] \quad (11a,b)$$

where $[\text{PLB}_{tot}]$ and $[\text{SERCA}_{tot}]$ are the concentrations of PLB and SERCA added during reconstitution, respectively. [PLB] in eq 9 can then be expressed using a quadratic equation in terms of total protein concentrations

$$[\text{PLB}] = \frac{-b + (b^2 - 4ac)^{1/2}}{2a} \quad (12)$$

with coefficients $a = 1$, $b = [\text{SERCA}_{tot}] - [\text{PLB}_{tot}] + K_{d2}$, and $c = -K_{d2}[\text{PLB}_{tot}]$.

When all specific PLB binding sites on SERCA are occupied with acceptor-labeled PLB, FRET is equal to E_{max} and the fraction of SERCA molecules bound is equal to 1. Therefore, FRET due to specific binding at any fraction bound can be expressed as

$$E_{SB} = E_{max}\left(1 - \frac{[\text{SERCA}]}{[\text{SERCA}_{tot}]}\right) = E_{max}\left(1 - \frac{[\text{SERCA}_{tot}] - [\text{PLB}_{tot}] + [\text{PLB}]}{[\text{SERCA}_{tot}]}\right) \quad (13)$$

Specific binding interaction between donor-labeled SERCA and acceptor-labeled PLB was analyzed using eq 13 (right side) substituted with eq 12.

When the fraction of SERCA molecules bound is equal to 1, the distance between the donor and acceptor in each complex should be the same, assuming homogeneity in complex formation. Therefore, E_{max} was used to calculate the donor−acceptor distance R (eq 3).

Analysis of Nonspecific FRET. In addition to the FRET caused by specific binding of PLB, to SERCA, we calculated the additional FRET due to the random arrangement of acceptor-labeled PLB in the membrane. As described by Fung and Stryer (*49*), this FRET depends on the concentration of acceptors in the membrane, and on the distance of closest approach (R_c) between the donor and acceptor. An approximate version of this theory, which is accurate when

$R_c \geq 0.7R_o$, can be expressed in the form of the Stern−Volmer equation (*50*):

$$\frac{F_{SB}}{F_{SB+NS}} = 1 + K_Q[PLB_{tot}] \quad (14)$$

where F_{SB} and F_{SB+NS} are fluorescence donor intensities after quenching by acceptor due to specific binding alone (F_{SB}) and due to both specific *and* nonspecific FRET (SB + NS), which are assumed to be independent processes. K_Q is the quenching constant that is dependent on R_c and R_o:

$$K_Q = \frac{\pi R_o^{\,6}}{2R_c^{\,4}} \quad (15)$$

Since E is the fractional decrease in donor fluorescence, total FRET observed (E_{tot}) is given by combining eqs 13 and 14

$$E_{tot} = \frac{(E_{max}(1 + [PLB]) + K_Q[PLB_{tot}])}{(1 + K_Q[PLB_{tot}])} \quad (16)$$

with eq 12 substituted for [PLB]. The data sets, obtained at different values of [PLB_{tot}], were fit globally to eq 16, in a nonlinear least-squares analysis, to determine the values of K_Q, K_{d2}, and E_{max}.

Time-Resolved Phosphorescence Anisotropy. Purified SERCA was labeled with the phosphorescent dye ErITC as described previously (*29*, *51*). Preparation of SERCA in a membrane environment and removal of unreacted dye were identical to the method used for fluorescent labeling. Labeled SERCA was co-reconstituted with varying amounts of I40A-PLB, exactly as described above for FRET samples, to measure SERCA aggregation using TPA. Data were acquired and analyzed as described previously (*29*).

Western Blot Analysis of Reconstituted Samples. Reconstituted samples were solubilized in 0.01% Tween, and electrophoresed (*52*) on a 4−20% Tris−glycine precast Criterion gel (Biorad) to separate proteins from lipid. Following electrophoresis, proteins were transferred to poly(vinylidene difluoride) (PVDF) membranes using the Criterion western blot instrumentation setup in transfer buffer (190 mM glycine, 10% methanol by volume, 0.01% SDS, 25 mM Tris−base, pH not adjusted) at 4 °C. The gel was then stained with Coomassie Blue to detect any residual protein, and transfer conditions were optimized so that complete transfer of protein to the PVDF membrane occurred. Once transferred completely, the membrane was incubated overnight in blocking buffer (2% nonfat dry milk in wash buffer containing 0.2 M NaCl, 0.01% Tween, and 50 mM Tris−base, pH 7.4) at 4 °C with shaking. After the membrane was washed three times for 10 min in wash buffer, the blot was incubated with primary antibody 8A3-D5 (diluted 1:1500 in blocking buffer) for 1 h at room temperature with shaking, followed by three more washing cycles. The blot was then incubated for 1 h at room temperature with [I^{125}]protein A (diluted 1:500 in blocking buffer) and washed three more times. The PVDF membrane was air-dried, wrapped in plastic foil, and exposed using a Kodak phosphor screen. The blot was quantitated on a Storm PhosphorImager (Amersham Biosciences, Piscataway, NJ). Standards consisted of the same purified DAB−I40A-PLB that was used for reconstitution.

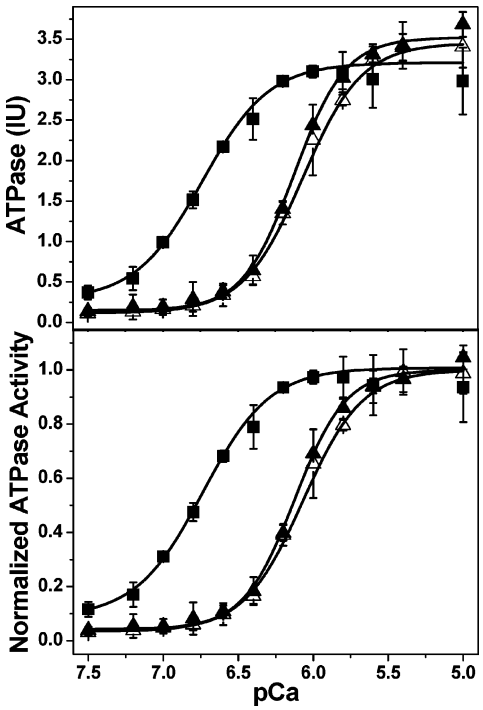

FIGURE 2: Activity of SERCA reconstituted alone (■), and with unlabeled I40A-PLB (▲) or DAB−I40A-PLB (△). Curves show the best fits to eq 1. Top: raw data expressed in IUs [(μmol of ATP/mg of protein)/min]. Bottom: data normalized to V_{max} of the fit to eq 1. Values are the mean ± standard deviation of three experiments conducted at 25 °C using an NADH-linked assay.

RESULTS

Characterization of Labeled Proteins. The dye-to-protein molar ratio of AEDANS−SERCA was calculated to be 0.95 ± 0.09. The labeled enzyme, reconstituted into lipid membranes, retained 70−80% of its Ca-dependent ATPase activity and all of its sensitivity to regulation by PLB. Mass spectrometry of DAB−I40A-PLB confirmed that both synthesis and labeling were successful and yielded the correct product. The major peak of mass spectrometry was at 6330.50 Da [M + H] (theoretical: 6333.94 Da), confirming that the peptide was synthesized completely, with a DABCYL molecule bound to the terminal amino group of Lys 3. Analysis of unlabeled, acetylated I40A-PLB showed a major peak at 6080.0 Da [M + H] (theoretical: 6081.54 Da). Amino acid analysis was consistent with the expected peptide composition. Results from amino acid analysis and direct sample absorbance verified a dye-to-protein ratio of 0.98 ± 0.1.

To determine the effect of the DABCYL label on I40A-PLB inhibitory function, purified SERCA was co-reconstituted with either unlabeled I40A-PLB or DAB−I40A-PLB at a membrane concentration of 1.4 SERCAs/1000 lipids and 10 PLBs/SERCA (mol/mol). SERCA ATPase activity (Figure 2) was determined using an NADH-linked enzymatic assay (*32*, *43*). SERCA reconstituted alone exhibited the expected Ca sensitivity, with a half-maximal pCa value (pK_{Ca} in eq 1) of 6.81 ± 0.02, and a maximal ATPase activity (V_{max} in eq 1) of 3.21 ± 0.06 IUs (μmol of ATP mg^{-1} min^{-1})

at micromolar free Ca. Unlabeled I40A-PLB decreased the apparent Ca affinity of SERCA as expected, to $pK_{Ca} = 6.12 \pm 0.02$ when co-reconstituted with unlabeled I40A-PLB (*43*). The labeling of I40A-PLB with DABCYL-SE on Lys 3 had no effect on the inhibitory activity of I40A-PLB (Figure 2). The rightward shift of the Ca activation curve caused by labeled I40A-PLB (to $pK_{Ca} = 6.11 \pm 0.02$) was essentially identical to that of unlabeled I40A-PLB. The label also had no effect on the shape of the curve; the Hill coefficient in the presence of labeled I40A-PLB (2.08 ± 0.15; n in eq 7) indicated cooperativity, as did those obtained for the control (1.70 ± 0.14) and with unlabeled I40A-PLB (2.07 ± 0.15). Maximal ATPase activity ($V_{max} = 3.62 \pm 0.10$ IUs with unlabeled I40A-PLB) was essentially unaffected by the label (3.48 ± 0.07 IUs). Therefore, DAB−I40A-PLB is suitable for studying the binding interaction of SERCA and PLB in a functional membrane system. At pCa 6.5 (low Ca), the total inhibition of SERCA by either unlabeled or labeled I40A-PLB is greater than 80% (Figure 2). At pCa 5.0 (high Ca), there is no inhibition by either labeled or unlabeled I40A-PLB.

Western Blots of Reconstituted Samples. When a dissociation constant is measured, it is necessary to obtain an accurate measurement of the concentration of ligand present. It has been reported previously (*26*, *40*), using a different reconstitution method that involves a centrifugation step and a greater amount of Biobeads, that PLB can be lost during the reconstitution procedure. Therefore, Western blot analysis of reconstituted samples was conducted to determine whether PLB was lost during reconstitution. We used anti-PLB antibody 8A3-D5 and purified DAB-I40A-PLB as standard (concentration determined using amino acid analysis). The detection range of this method was linear from 0 to 100 ng of PLB, and samples were diluted so that this range was not exceeded. Control experiments with lipids and SERCA showed that antibody detected only PLB, and was not altered by lipids or SERCA. We determined that the PLB content of the reconstituted samples used for fluorescence and activity measurements was quantitatively identical to the initial content. We conclude that the protein compositions of the reconstituted samples are accurate.

Fluorescence Data Analysis. FRET measurements were conducted on co-reconstituted samples containing AEDANS−SERCA (SERCA from here on) and DAB−I40A-PLB (PLB from here on). Both the ratios of these proteins and their respective membrane concentrations were varied to measure the dependence of binding on protein concentrations in the membrane. The amount of PLB present in the membrane was adjusted for incorrectly oriented PLB (facing into the vesicle, away from the SERCA cytoplasmic domain). In reconstituted samples, the SERCA enzyme is oriented asymmetrically, with the cytoplasmic domains protruding from the vesicle, while PLB is oriented symmetrically, with approximately half of the molecules oriented right-side-out, and the other half inverted (*53*). SERCA interacts preferentially with correctly oriented PLB (*26*). Furthermore, if the acceptor-labeled cytoplasmic domain of PLB is on the opposite side of the membrane from the donor-labeled cytoplasmic domain of SERCA, the distance between the donor and acceptor is too great (greater than 60 Å) for these pairs to participate in FRET. Therefore, incorrectly oriented PLB is not part of either the biochemical or the spectroscopic

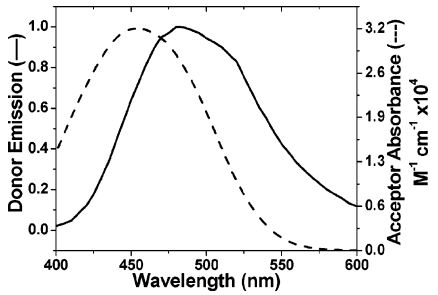

FIGURE 3: Moderate spectral overlap of donor AEDANS emission (−) and acceptor DABCYL absorbance (---). The donor site is SERCA Cys 674, and the acceptor site is PLB Lys 3. The Förster distance for this dye pair is 32 Å (*45*).

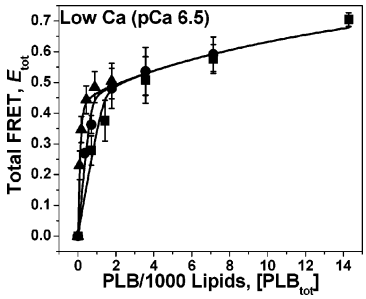

FIGURE 4: Total FRET at low Ca (pCa 6.5) due to SERCA−PLB interaction as a function of the total membrane concentration of PLB. SERCA membrane concentrations were 1.4 (■), 0.71 (●), and 0.18 (▲) SERCA/1000 lipids. Experiments were conducted at 25 °C, in buffer containing 50 mM KCl, 5 mM $MgCl_2$, 50 mM MOPS (pH 7.0), 0.5 mM EGTA, and 210 μM $CaCl_2$. Data points represent the mean ± standard deviation of two or more experiments. Curves show the best fits of eq 16.

data sets collected here, and the amount of correctly oriented PLB participating in inhibition and FRET is half of that added during reconstitution. All data were corrected accordingly.

Spectral overlap of donor emission and acceptor absorbance (Figure 3) is moderate, and the dye pair has a Förster distance (eq 4) of 32 Å (*45*). Thus, at distances greater than 45 Å, the FRET contribution is less than 10%. The dimensions of a SERCA molecule are 55−90 Å across the cytoplasmic domains (*54*, *55*), so FRET is only detectable when the proteins actually interact physically in the membrane, and FRET dissipates quickly as soon as PLB dissociates from the enzyme. For the same reason, contribution to FRET by acceptors bound to inverted PLB molecules (across the membrane) is also insignificant.

FRET at Low Ca (pCa 6.5). Steady-state FRET (eq 2) was measured at low Ca (pCa 6.5) in co-reconstituted membranes from SERCA to PLB (Figure 4). The PLB/SERCA ratio was varied from 0 to 20, and the membrane concentration of SERCA ranged from 1.4 to 0.18 SERCA/1000 lipids. Energy transfer increased sharply upon addition of PLB, and began to change more gradually when the expected stoichiometry of the complex was exceeded. The curves did not overlap at low [PLB_{tot}], but only at PLB membrane concentrations of greater than 2 PLBs/1000 lipids. Nonspecific FRET, which could be well described by the model based on the Fung and Stryer theory (*49*), became prevalent when the PLB concentration in the membrane exceeded 2 PLBs/1000 lipids, likely after formation of a SERCA−PLB complex was virtually complete. Total FRET did not approach a maximal value but continued to increase

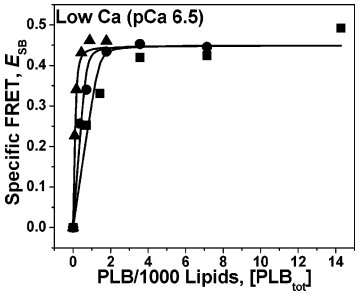

FIGURE 5: FRET at low Ca (pCa 6.5) due to SERCA−PLB interaction as a function of the total membrane concentration of PLB corrected for the nonspecific component. SERCA membrane concentrations were 1.4 (■), 0.71 (●), and 0.18 (▲) SERCA/1000 lipids. Experiments were conducted at 25 °C, in buffer containing 50 mM KCl, 5 mM $MgCl_2$, 50 mM MOPS (pH 7.0), 0.5 mM EGTA, and 210 μM $CaCl_2$. Curves show the best fits of eq 16 after correction for the nonspecific component determined from the fit shown in Figure 4.

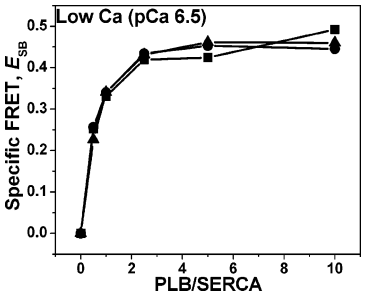

FIGURE 6: FRET due to specific SERCA−PLB interaction at low Ca (pCa 6.5) as a function of the ratio of total PLB to SERCA in the membrane at SERCA membrane concentrations of 1.4 (■), 0.71 (●), and 0.18 (▲) SERCA/1000 lipids. Experiments were conducted at 25 °C, in buffer containing 50 mM KCl, 5 mM $MgCl_2$, 50 mM MOPS (pH 7.0), 0.5 mM EGTA, and 210 μM $CaCl_2$.

with the membrane concentration of PLB. According to the fit, the distance of closest approach R_c was 26 ± 3 Å (eq 15). This validates the use of the simplified theory for nonspecific FRET in the membrane (eq 14), since R_c is greater than $0.7R_o$ (*50*). By fitting of eq 16, it was possible to resolve nonspecific FRET from the specific component that depends on the dissociation equilibrium (eq 7).

FRET binding curves were corrected for nonspecific FRET as determined by the fits of eq 16, and replotted as specific FRET (E_{SB}) (Figure 5). When the dissociation constant was linked in the global analysis ($\chi^2 = 8.6E-4$), K_{d2} was 0.018 ± 0.012 PLB/1000 lipids. This indicates that the binding was at such high affinity that this K_{d2} value should be considered an upper bound for the actual K_{d2}. *Thus, in the PLB concentration range studied here, the specific binding of PLB to SERCA is essentially stoichiometric*. Therefore, the specific FRET data should be replotted as E_{SB} vs the ratio of ligand (PLB) to enzyme (SERCA).

Specific FRET data at low Ca (pCa 6.5) were replotted as a function of the ratio of total PLB to SERCA in the membrane (Figure 6). The curves now overlap at all SERCA membrane concentrations. *This indicates tight stoichiometric binding, with K_{d2} much lower than the concentration of PLB in the membrane used in these experiments, which in turn is much lower than the physiological concentration of PLB in cardiac SR membranes* (*56*). It was not possible to attenuate this high-affinity specific binding by dilution of the proteins in the membrane.

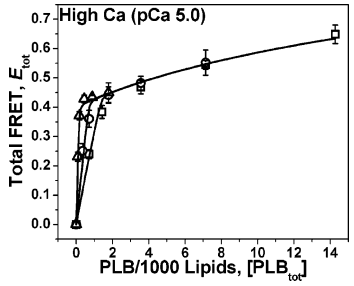

FIGURE 7: Total FRET due to SERCA−PLB interaction at high Ca (pCa 5.0) as a function of the ratio of total PLB to SERCA in the membrane at SERCA membrane concentrations of 1.4 (□), 0.71 (○), and 0.18 (Δ) SERCA/1000 lipids. Experiments were conducted at 25 °C, in buffer containing 50 mM KCl, 5 mM $MgCl_2$, 50 mM MOPS (pH 7.0), 0.5 mM EGTA, and 489 μM $CaCl_2$. Curves show the best global fits of eq 16.

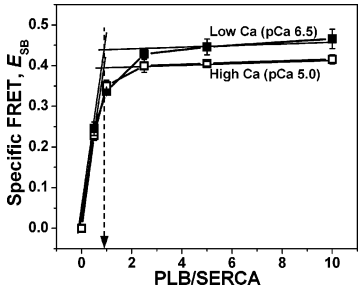

FIGURE 8: Specific FRET due to specific binding interaction between SERCA and PLB. Data represent the mean ± standard deviation of all SERCA membrane concentrations at pCa 6.5 (■) and pCa 5.0 (□). The stoichiometry of the SERCA−PLB complex is 1:1 at both low and high Ca (indicated by a dashed arrow). The change in E_{max} may be attributed to a small structural change in the complex with respect to the donor−acceptor distance in transition from low to high Ca.

FRET at High Ca (pCa 5.0). Having established that binding of PLB to SERCA at low Ca is of very high affinity and stoichiometric in nature, we conducted FRET experiments at pCa 5.0 with the same samples, to test the hypothesis that the SERCA−PLB complex dissociates at high Ca due to an increase in K_{d2} (Figure 1). Surprisingly, the FRET results at high Ca (Figure 7) were nearly identical to those obtained at low Ca (Figure 4), suggesting that high-affinity binding occurred at high Ca in the same manner as that at low Ca. The nonspecific FRET component was observed at PLB membrane concentrations of greater than 2 PLBs/1000 lipids, where it was also observed at low Ca. The distance of closest approach (R_c = 27 ± 2 Å), and therefore the quality of nonspecific quenching, was virtually identical to that at low Ca ($R_c = 26 \pm 3$ Å). After correction for nonspecific FRET, the remaining FRET due to specific binding interaction was essentially identical at all SERCA membrane concentrations, and the stoichiometric (extremely-high-affinity) binding observed at low Ca was therefore also observed at high Ca.

Stoichiometry of the SERCA−PLB Complex. FRET due to specific binding only depended on the ratio of total PLB to SERCA in the membrane (Figure 8) at both low and high Ca. The stoichiometry of the complex was determined by extrapolating straight lines from the slope of initial and final data points. As indicated by the dashed arrow in Figure 8, the stoichiometry of the PLB−SERCA complex in a functional membrane system is 1.0 ± 0.1 PLB/SERCA under both activating and inhibitory Ca concentrations.

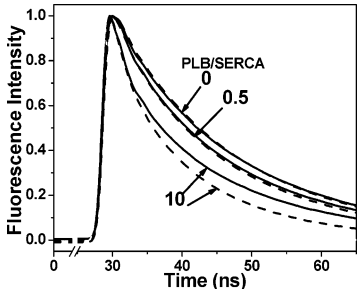

FIGURE 9: Time-resolved FRET decays due to SERCA−PLB interaction at low Ca (pCa 6.5) as a function of the molar ratio of PLB to SERCA. SERCA membrane concentrations were 1.4 (---) and 0.18 (−) SERCA/1000 Lipids. Experiments were conducted under conditions identical to those of steady-state experiments (Figure 4). Decays are representative of those collected at high Ca (pCa 5.0).

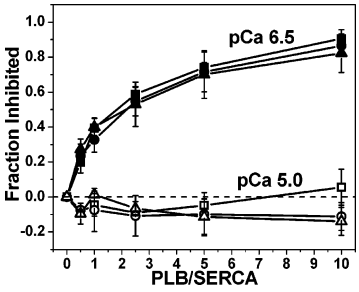

FIGURE 10: Fraction of SERCA activity inhibited by PLB at low Ca (pCa 6.5; ■, ●, ▲) and high Ca (pCa 5.0; □, ○, △) at SERCA membrane concentrations of 1.4 (■, □), 0.71 (●, ○), and 0.18 (▲, △) SERCA/1000 lipids. Activity was measured using an NADH-linked ATPase assay at 25 °C in microtiter plates. Data represent the mean ± standard deviation of two or more experiments using the same samples used for FRET experiments.

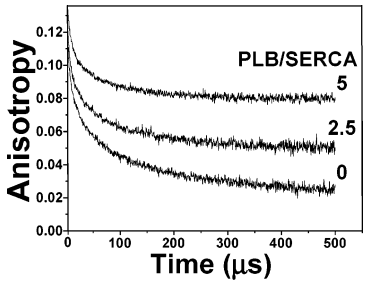

FIGURE 11: Time-resolved phosphorescence anisotropy of ErITC−SERCA co-reconstituted with I40A-PLB at 1.4 SERCAs/1000 lipids. Experiments were conducted under conditions similar to those of Figure 6.

When specific FRETs due to specific binding were compared at low and high Ca (Figure 8), a small but significant difference in maximal energy transfer (obtained from fitting of eq 16) was noted. E_{max} was 0.45 ± 0.02 at low Ca, and 0.40 ± 0.01 at high Ca. On the basis of the Förster distance of 32 Å (Figure 3) and using eq 3, this corresponds to a distance of 33.1 ± 0.4 and 34.2 ± 0.2 Å at low and high Ca, respectively. Therefore, with respect to the donor−acceptor distance of the labeling sites used here, there was a *small but significant structural change in the complex in the transition from low to high Ca*. It is clear, however, that the complex did not dissociate at high Ca, as shown by saturation of specific FRET at both low and high Ca.

Time-Resolved Fluorescence Analysis. We conducted time-resolved fluorescence experiments on the same samples to confirm and clarify the findings. Time-resolved data supported the findings of steady-state analysis at both low and high Ca concentration. Average fluorescence lifetimes of decays were consistent with steady-state FRET data. The SERCA membrane concentration did not affect the average decay in the absence of PLB, shown by essentially identical decays at 1.4 and 0.18 SERCA/1000 lipids (Figure 9). Upon addition of 0.5 PLB/SERCA, fluorescence decayed faster than in the absence of PLB, indicating FRET, and the decays from two different SERCA membrane concentrations were identical, supporting the conclusion from steady-state data that the interaction is stoichiometric and specific at this low ratio of PLB to SERCA (Figure 8). At an excess of PLB over SERCA, the decay at 1.4 SERCAs/1000 lipids was clearly faster than that at 0.18 SERCA/1000 lipids (Figure 9), consistent with the presence of more nonspecific FRET at the former and less at the latter SERCA concentration. When eq 6 was fitted to the data, it was generally found that more exponentials were needed for satisfactory fits at higher SERCA membrane concentration, suggesting that the nonspecific FRET observed under these conditions arises from a distribution of distances between the donor and acceptor due to nonspecific binding of PLB to SERCA. These results confirm the above interpretation of steady-state FRET.

ATPase Activity. SERCA ATPase activity (Figure 10) was measured on the same reconstituted and labeled samples that were used for fluorescence measurements at pCa 6.5 and 5.0. At pCa 6.5, PLB inhibits SERCA, whereas there is no inhibition at pCa 5.0 (Figure 2). No inhibition of SERCA by PLB was observed at pCa 5.0, as expected. In fact, there was a slight increase in activity in the presence of PLB at pCa 5.0, as reported previously (*43*). At pCa 6.5, SERCA ATPase activity was inhibited to the same extent at all SERCA membrane concentrations by PLB (Figure 10), suggesting that inhibition is dependent on the ratio of total PLB to SERCA, and not the membrane concentration of PLB, consistent with specific FRET measurements. Inhibition increased sharply upon addition of PLB, and continued to increase in stoichiometric fashion (curves overlapped) even beyond the 1:1 stoichiometry of the SERCA−PLB complex. This suggested the presence of a nonspecific component of inhibition.

TPA of SERCA Co-Reconstituted with I40A-PLB. To assess the role of SERCA self-association (K_{d3} in Figure 1) in the mechanism of PLB-dependent inhibition, we conducted TPA measurements of phosphorescent-labeled SERCA co-reconstituted with I40A-PLB (Figure 11). PLB caused significant increases in anisotropy, indicating SERCA aggregation, consistent with previous observations in cardiac SR (*30*). Although FRET showed that the specific binding interaction between SERCA and PLB is saturated at a ratio greater than 1 PLB/SERCA (Figure 8), TPA showed aggregation of SERCA that continued to increase in virtually linear fashion (on the basis of the final anisotropy evaluation) from 2.5 to 5 PLBs/SERCA added. This aggregation probably accounts for the continued increase in inhibition at high PLB/SERCA ratios (Figure 10).

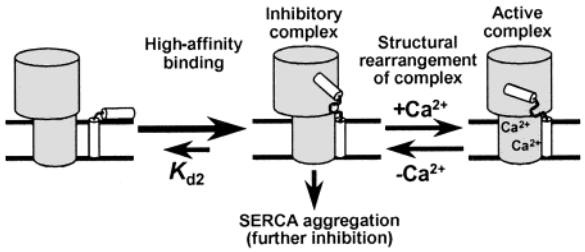

FIGURE 12: Partially revised model of SERCA−PLB interaction. Under physiological conditions, PLB is a subunit of SERCA that does not dissociate from the enzyme at saturating Ca^{2+} concentration. Instead, a structural rearrangement occurs in the SERCA−PLB complex to overcome inhibition. This is a revision of the illustration shown in Figure 1.

DISCUSSION

Summary. We have used FRET to detect directly the interaction between SERCA and PLB in a functional, Ca-sensitive, and biochemically coupled system of intact membranes. The same samples were used for both activity and fluorescence measurements, allowing for direct correlation of the structure and function of the SERCA−PLB complex in lipid bilayers of controlled protein and lipid composition. This produced well-defined thermodynamic conditions and allowed us to test directly the hypothesis that the relief of SERCA inhibition at high Ca^{2+} is due to the dissociation of PLB (Figure 1). We conclude that this hypothesis must be revised (Figure 12).

Tight, Ca-Independent Binding of PLB to SERCA. We have shown directly that the SERCA−PLB complex remains intact at saturating [Ca^{2+}]. FRET measurements showed that specific binding of PLB to SERCA at both inhibitory and activating [Ca^{2+}] is stoichiometric (Figure 8). I40A-PLB remained bound to SERCA at pCa 5.0 despite complete reversal of inhibition, so reversal of inhibition does not require dissociation of PLB. Co-immunoprecipitation of PLB with SERCA 1a or 2a (*21*) was reduced at saturating Ca concentration. However, the enzyme is inactive in the detergent conditions used, and correlation of physical and biochemical measurements is difficult. In the present study, done in functional membranes, Ca clearly relieves inhibition (Figure 10) without dissociating PLB from SERCA (Figures 7 and 8).

An 8-fold dilution of the proteins in the membrane (from a SERCA membrane concentration of 1.4 SERCAs/1000 lipids to one of 0.18 SERCA/1000 lipids) had no effect on the specific binding interaction: specific FRET as a function of the ratio of total PLB to SERCA was virtually identical at all SERCA membrane concentrations. Therefore, PLB binds to SERCA with *very* high affinity (Figure 12), with K_{d2} much lower than the membrane protein concentrations used in these experiments and therefore much lower than the physiological membrane concentrations of these proteins (*56*). Since binding was too tight to measure the dissociation constant, and since there is at least 1 PLB/SERCA in both slow-twitch skeletal and cardiac SR membranes (*56*−*59*), *we conclude that each SERCA molecule under normal physiological conditions has a PLB molecule specifically bound to it*. In effect, *all SERCA molecules are permanently under adrenergic control*, regardless of whether the interaction is strongly inhibitory (low Ca) or moderately activating (high Ca) (Figure 2). This serves as one mechanism of access to the large cardiac reserve in most animals. We propose therefore that, *under physiological conditions, PLB should be considered a subunit of SERCA* that is bound at both low (nanomolar) and high (micromolar) Ca^{2+} concentration (Figure 12).

It is conceivable that superinhibitory I40A-PLB binds to SERCA with greater affinity than WT-PLB, and that WT-PLB interactions with SERCA are decreased at high Ca. It is also possible that the labeled PLB has greater affinity for SERCA than does unlabeled PLB. If the PLB−PLB interaction were of comparable affinity to the PLB−SERCA interaction, equilibria involving K_{d1} and K_{d2} (Figure 1) would be in competition, and dissociation of the SERCA−PLB complex would be more likely. However, it has been shown that PLB oligomers dissociate in the presence of SERCA (*60*), indicating that the interaction between SERCA and the PLB monomer is dominant.

Other, less direct, evidence is consistent with Ca-independent binding of PLB to SERCA. Cross-linking experiments conducted under reportedly uncontrolled Ca conditions (*25*), and therefore presumably at saturating Ca concentration, detected proximity between PLB and SERCA. Infrared spectroscopy showed that the effects of PLB on SERCA were the same at low and high Ca (*26*).

Despite clear evidence for stoichiometric binding of PLB to SERCA, plots of specific FRET as a function of the ratio of total PLB to SERCA (Figure 8) display a degree of curvature. Since we conclude that the membrane concentration of PLB is much greater than K_{d2}, it is expected instead that a sharp kink should be observed at the point of stoichiometry of the SERCA−PLB complex (1:1) as illustrated by the straight lines in Figure 8. The most likely source of curvature is heterogeneity in the composition of vesicles, an artifact of reconstitution. Simulations of the data in Figure 8 indicate that the observed curvature can be accounted for by assuming that the actual ratio of PLB to SERCA in individual vesicles varies by about 30% within a single preparation. Curvature could also arise from aggregation of the enzyme (*18*, *27*−*30*), which is likely to produce a heterogeneous system in which some PLB binding sites are less accessible than others, or from cooperativity within a preexisting oligomeric SERCA complex (*46*, *61*).

The reconstitution system is optimal for measuring the binding of two membrane proteins under defined conditions, because membrane protein concentrations and ratios can be varied precisely. K_{d2} was previously estimated to be 0.22 PLB/1000 lipids (*26*) at a concentration comparable to 1.4 SERCAs/1000 lipids, whereas we obtain an upper bound for K_{d2} that is at least 10 times lower. This overestimate of K_{d2} is due to the failure to vary the membrane concentration of SERCA in that study (*26*), so it was not possible to detect the stoichiometric, high-affinity binding detected here.

Our results shed light on physical aspects of successful gene therapy targeting the SERCA−PLB system in hamsters (*15*), which attenuated progression to heart failure. During protein synthesis, SERCA and PLB are inserted into membranes, where they may become available for immediate interaction. Once PLB is bound to SERCA, the complex is unlikely to dissociate due to the very-high-affinity interaction. If, upon insertion into the membrane, a competing mutant of PLB is present that binds to SERCA first, WT-PLB may be permanently displaced from specific SERCA binding sites,

in effect preventing deleterious effects of PLB on SERCA implicated in heart failure (*3*−*9*).

SERCA−*PLB Complex Stoichiometry and Structure.* We have shown here that the stoichiometry of the SERCA−PLB complex is 1:1, consistent with most other models (i.e., refs *47* and *48*), including the model of two PLB molecules bound to a SERCA homodimer (*46*). The SERCA−PLB complex has been proposed to consist of one PLB molecule per SERCA dimer (*56*), but that model was based on an erroneously high estimate for the value of K_{d2} as explained above. The best estimate for the expected donor−acceptor distance in the Ca-free crystal structure is approximately 40 Å (SERCA Cys 674 to Lys 400; on the basis of PLB Lys 3 cross-linking to SERCA residues 397−400; *22*). The distance measured with FRET in the present study is approximately 7 Å shorter; this difference can easily be accounted for by structural dynamics, uncertainty of probe conformations, or the distance separating PLB Lys 3 from SERCA Lys 400 that was probably bridged by the cross-linker (*22*). The observed distance is not consistent with the hypothesis that PLB binds to SERCA with its cytoplasmic domain in contact with the membrane surface; rather, our observations are consistent with the conclusion that SERCA induces a large conformational change in PLB, lifting the cytoplasmic domain substantially above the membrane surface (*62*).

Ca-Dependent Structural Change within the SERCA−*PLB Complex.* What does happen when [Ca^{2+}] relieves inhibition? Our results show that the maximum energy transfer efficiency at saturating PLB (E_{max}) is significantly less at high Ca (Figure 8), indicating a *structural change within the SERCA*−*PLB complex induced by micromolar* Ca^{2+}. This is consistent with the evidence from spectroscopy (*63*) and from crystallography (*54*, *55*) that there is a substantial conformational change within SERCA in the transition from low to high Ca. On the basis of the change in E_{max}, the donor−acceptor distances at low and high Ca (33.1 ± 0.4 and 34.2 ± 0.2 Å, respectively) display a small but significant change. This is consistent with the small change predicted in the distance between Cys 674 and Lys 400, from the Ca-bound to the Ca-free SERCA crystal structures (*54*, *55*). A larger change, more characteristic of large domain movements thought to occur during the SERCA enzymatic cycle (i.e., refs *54*, *55*, and *64*), would presumably be detected with a donor probe at another site on SERCA. Conformational changes in the SERCA−PLB complex upon Ca binding probably explain the observed Ca-dependent cross-linking of PLB to the enzyme (*22*−*24*). For cross-linking to occur efficiently, distances between sites must match the length of the cross-linker, and alignment of residues to be cross-linked must be sterically favorable. Rotational or translational helix or domain movement containing the cross-linking residues may be sufficient to prevent cross-linking if the distance between sites becomes too great or short, alignment of the residues is unfavorable, or at least one of the residues becomes inaccessible to the cross-linker due to steric hindrance. Cross-linking was surprisingly dependent on the presence of nucleotide (*23*, *24*), which may induce SERCA conformations that favor cross-linking to PLB.

Nonspecific Binding and Inhibition. FRET measurements showed a nonspecific component that became prevalent at PLB membrane concentrations that exceeded the stoichiometry of the SERCA−PLB complex (Figures 4 and 7), and this was accounted for by assuming random arrangement of PLB in the membrane (*49*). Proximity to various acceptors at a range of distances would give rise to numerous different energy-transfer events, and this was confirmed by the complexity of time-resolved fluorescence decays (Figure 9). Nonspecific FRET may also arise due to SERCA aggregation (Figure 11), which has been shown previously to occur in the presence of PLB and other inhibitors (*18*, *27*−*30*). Acceptor-labeled PLB may become trapped in nonspecific sites that lead to FRET, in addition to specifically bound PLB. This is more likely to occur at high protein concentrations in crowded membranes. After correction for the nonspecific FRET component, all remaining FRET overlapped, indicating high-affinity, stoichiometric binding due to a specific interaction (Figure 8).

SERCA aggregation (Figure 11) probably helps to explain some of the complexity in the inhibition data (Figure 10). A correlation between aggregation and inhibition is observed upon addition of PLB (*30*) and other inhibitors (*27*−*29*, *65*−*68*), some of which are likely to be nonspecific. Aggregation probably serves as part of the mechanism of control of SERCA activity by PLB. It is clear from Figure 10 that there are remaining interactions that are not detected by FRET, but still cause inhibition. The various inhibitory mechanisms of PLB on SERCA are likely to be more complex than can be detected here, and deserve further attention.

Conclusions and Future Work. We have shown that FRET can be used to detect and quantitate the binding interaction of PLB and SERCA in intact membranes, and that this interaction is so strong that PLB is effectively a subunit of the SERCA enzyme under physiological conditions. The SERCA−PLB complex has a stoichiometry of 1:1 in a functional membrane system at both activating and inhibitory Ca concentrations. While micromolar Ca^{2+} does not dissociate PLB from SERCA, our FRET data strongly suggest that it does change the structure of the SERCA−PLB complex, and this internal structural change is probably the mechanism by which inhibition is relieved. Further experiments will be needed to understand the effects of nucleotide, phosphorylation, and mutation on the structure of the SERCA−PLB complex.

ACKNOWLEDGMENT

We thank Dr. John Lipscomb for helpful discussions about binding data analysis and interpretation. Drs. Gregory Hunter, Laxma Reddy, and Anne Walter provided insightful advice during the early phases of this project. Drs. James Mahaney and Diana Bigelow also provided helpful advice. Zhiwen Zhang and Sara Ehrlich provided excellent technical assistance with biochemical preparations and analysis. Thomas Krick and Dr. LeeAnn Higgins assisted in the Facility for Mass Spectrometry in the Life Sciences (University of Minnesota), and Jinny Johnson and Dr. Lawrence Dangott conducted amino acid analysis and protein sequencing at the Protein Chemistry Laboratory (Texas A&M University, College Station, TX). We thank Dr. G. Gillispie and T. Martin at Dakota Technologies, Inc., for assistance in constructing and operating the time-resolved fluorescence spectrometer.

REFERENCES

1. Tada, M., Kadoma, M., Fujii, J., Kimura, Y., and Kijima, Y. (1989) Molecular structure and function of phospholamban: the regula-

tory protein of calcium pump in cardiac sarcoplasmic reticulum, *Adv. Exp. Med. Biol. 255*, 79−89.
2. Sham, J. S., Jones, L. R., and Morad, M. (1991) Phospholamban mediates the beta-adrenergic-enhanced Ca^{2+} uptake in mammalian ventricular myocytes, *Am. J. Physiol. 261*, H1344−9.
3. Dhalla, N. S., Panagia, V., Singal, P. K., Makino, N., Dixon, I. M., and Eyolfson, D. A. (1988) Alterations in heart membrane calcium transport during the development of ischemia-reperfusion injury, *J. Mol. Cell. Cardiol. 20* (Suppl. 2), 3−13.
4. Minamisawa, S., Hoshijima, M., Chu, G., Ward, C. A., Frank, K., Gu, Y., Martone, M. E., Wang, Y., Ross, J., Jr., Kranias, E. G., Giles, W. R., and Chien, K. R. (1999) Chronic phospholamban-sarcoplasmic reticulum calcium ATPase interaction is the critical calcium cycling defect in dilated cardiomyopathy, *Cell 99*, 313−22.
5. Minamisawa, S., Sato, Y., Tatsuguchi, Y., Fujino, T., Imamura, S., Uetsuka, Y., Nakazawa, M., and Matsuoka, R. (2003) Mutation of the phospholamban promoter associated with hypertrophic cardiomyopathy, *Biochem. Biophys. Res. Commun. 304*, 1−4.
6. Movsesian, M. A., Bristow, M. R., and Krall, J. (1989) Ca^{2+} uptake by cardiac sarcoplasmic reticulum from patients with idiopathic dilated cardiomyopathy, *Circ. Res. 65*, 1141−4.
7. Sande, J. B., Sjaastad, I., Hoen, I. B., Bokenes, J., Tonnessen, T., Holt, E., Lunde, P. K., and Christensen, G. (2002) Reduced level of serine(16) phosphorylated phospholamban in the failing rat myocardium: a major contributor to reduced SERCA2 activity, *Cardiovasc. Res. 53*, 382−91.
8. Haghighi, K., Kolokathis, F., Pater, L., Lynch, R. A., Asahi, M., Gramolini, A. O., Fan, G. C., Tsiapras, D., Hahn, H. S., Adamopoulos, S., Liggett, S. B., Dorn, G. W., II, MacLennan, D. H., Kremastinos, D. T., and Kranias, E. G. (2003) Human phospholamban null results in lethal dilated cardiomyopathy revealing a critical difference between mouse and human, *J. Clin. Invest. 111*, 869−76.
9. Movsesian, M. A., Colyer, J., Wang, J. H., and Krall, J. (1990) Phospholamban-mediated stimulation of Ca^{2+} uptake in sarcoplasmic reticulum from normal and failing hearts, *J. Clin. Invest. 85*, 1698−702.
10. Schmitt, J. P., Kamisago, M., Asahi, M., Li, G. H., Ahmad, F., Mende, U., Kranias, E. G., MacLennan, D. H., Seidman, J. G., and Seidman, C. E. (2003) Dilated cardiomyopathy and heart failure caused by a mutation in phospholamban, *Science 299*, 1410−3.
11. Zhao, W., Frank, K. F., Chu, G., Gerst, M. J., Schmidt, A. G., Ji, Y., Periasamy, M., and Kranias, E. G. (2003) Combined phospholamban ablation and SERCA1a overexpression result in a new hyperdynamic cardiac state, *Cardiovasc. Res. 57*, 71−81.
12. Luo, W., Grupp, I. L., Harrer, J., Ponniah, S., Grupp, G., Duffy, J. J., Doetschman, T., and Kranias, E. G. (1994) Targeted ablation of the phospholamban gene is associated with markedly enhanced myocardial contractility and loss of beta-agonist stimulation, *Circ. Res. 75*, 401−9.
13. Lorenz, J. N., and Kranias, E. G. (1997) Regulatory effects of phospholamban on cardiac function in intact mice, *Am. J. Physiol. 273*, H2826−31.
14. Schmidt, A. G., Edes, I., and Kranias, E. G. (2001) Phospholamban: a promising therapeutic target in heart failure?, *Cardiovasc. Drugs Ther. 15*, 387−96.
15. Hoshijima, M., Ikeda, Y., Iwanaga, Y., Minamisawa, S., Date, M. O., Gu, Y., Iwatate, M., Li, M., Wang, L., Wilson, J. M., Wang, Y., Ross, J., Jr., and Chien, K. R. (2002) Chronic suppression of heart-failure progression by a pseudophosphorylated mutant of phospholamban via in vivo cardiac rAAV gene delivery, *Nat. Med. 8*, 864−71.
16. Cornea, R. L., Jones, L. R., Autry, J. M., and Thomas, D. D. (1997) Mutation and phosphorylation change the oligomeric structure of phospholamban in lipid bilayers, *Biochemistry 36*, 2960−7.
17. Kimura, Y., Kurzydlowski, K., Tada, M., and MacLennan, D. H. (1997) Phospholamban inhibitory function is activated by depolymerization, *J. Biol. Chem. 272*, 15061−4.
18. Thomas, D. D., Reddy, L. G., Karim, C. B., Li, M., Cornea, R., Autry, J. M., Jones, L. R., and Stamm, J. (1998) Direct spectroscopic detection of molecular dynamics and interactions of the calcium pump and phospholamban, *Ann. N. Y. Acad. Sci. 853*, 186−94.
19. MacLennan, D. H., and Kranias, E. G. (2003) Phospholamban: a crucial regulator of cardiac contractility, *Nat. Rev. Mol. Cell. Biol. 4*, 566−77.
20. MacLennan, D. H., Kimura, Y., and Toyofuku, T. (1998) Sites of regulatory interaction between calcium ATPases and phospholamban, *Ann. N. Y. Acad. Sci. 853*, 31−42.
21. Asahi, M., McKenna, E., Kurzydlowski, K., Tada, M., and MacLennan, D. H. (2000) Physical interactions between phospholamban and sarco(endo)plasmic reticulum Ca^{2+}-ATPases are dissociated by elevated Ca^{2+}, but not by phospholamban phosphorylation, vanadate, or thapsigargin, and are enhanced by ATP, *J. Biol. Chem. 275*, 15034−8.
22. James, P., Inui, M., Tada, M., Chiesi, M., and Carafoli, E. (1989) Nature and site of phospholamban regulation of the Ca^{2+} pump of sarcoplasmic reticulum, *Nature 342*, 90−2.
23. Chen, Z., Stokes, D. L., Rice, W. J., and Jones, L. R. (2003) Spatial and dynamic interactions between phospholamban and the canine cardiac Ca^{2+} pump revealed with use of heterobifunctional cross-linking agents, *J. Biol. Chem. 278*, 48348−56.
24. Jones, L. R., Cornea, R. L., and Chen, Z. (2002) Close proximity between residue 30 of phospholamban and cysteine 318 of the cardiac Ca^{2+} pump revealed by intermolecular thiol cross-linking, *J. Biol. Chem. 277*, 28319−29.
25. Young, E. F., McKee, M. J., Ferguson, D. G., and Kranias, E. G. (1989) Structural characterization of phospholamban in cardiac sarcoplasmic reticulum membranes by cross-linking, *Membr. Biochem. 8*, 95−106.
26. Tatulian, S. A., Chen, B., Li, J., Negash, S., Middaugh, C. R., Bigelow, D. J., and Squier, T. C. (2002) The inhibitory action of phospholamban involves stabilization of alpha-helices within the Ca-ATPase, *Biochemistry 41*, 741−51.
27. Mersol, J. V., Kutchai, H., Mahaney, J. E., and Thomas, D. D. (1995) Self-association accompanies inhibition of Ca-ATPase by thapsigargin, *Biophys. J. 68*, 208−15.
28. Karon, B. S., Geddis, L. M., Kutchai, H., and Thomas, D. D. (1995) Anesthetics alter the physical and functional properties of the Ca-ATPase in cardiac sarcoplasmic reticulum, *Biophys. J. 68*, 936−45.
29. Kutchai, H., Geddis, L. M., Jones, L. R., and Thomas, D. D. (1998) Differential effects of general anesthetics on the quaternary structure of the Ca-ATPases of cardiac and skeletal sarcoplasmic reticulum, *Biochemistry 37*, 2410−21.
30. Voss, J., Jones, L. R., and Thomas, D. D. (1994) The physical mechanism of calcium pump regulation in the heart, *Biophys. J. 67*, 190−6.
31. Karim, C. B., Marquardt, C. G., Stamm, J. D., Barany, G., and Thomas, D. D. (2000) Synthetic null-cysteine phospholamban analogue and the corresponding transmembrane domain inhibit the Ca-ATPase, *Biochemistry 39*, 10892−7.
32. Karim, C. B., Paterlini, M. G., Reddy, L. G., Hunter, G. W., Barany, G., and Thomas, D. D. (2001) Role of cysteine residues in structural stability and function of a transmembrane helix bundle, *J. Biol. Chem. 276*, 38814−9.
33. Lockwood, N. A., Tu, R. S., Zhang, Z., Tirrell, M. V., Thomas, D. D., and Karim, C. B. (2003) Structure and function of integral membrane protein domains resolved by peptide-amphiphiles: application to phospholamban, *Biopolymers 69*, 283−92.
34. Tarr, G. E., Black, S. D., Fujita, V. S., and Coon, M. J. (1983) Complete amino acid sequence and predicted membrane topology of phenobarbital-induced cytochrome P-450 (isozyme 2) from rabbit liver microsomes, *Proc. Natl. Acad. Sci. U.S.A. 80*, 6552−6.
35. King, D. S., Fields, C. G., and Fields, G. B. (1990) A cleavage method which minimizes side reactions following Fmoc solid-phase peptide synthesis, *Int. J. Pept. Protein Res. 36*, 255−66.
36. Arkin, I. T., Adams, P. D., Brunger, A. T., Aimoto, S., Engelman, D. M., and Smith, S. O. (1997) Structure of the transmembrane cysteine residues in phospholamban, *J. Membr. Biol. 155*, 199−206.
37. Stokes, D. L., and Green, N. M. (1990) Three-dimensional crystals of CaATPase from sarcoplasmic reticulum. Symmetry and molecular packing, *Biophys. J. 57*, 1−14.
38. Lowry, H., Rosenbrough, N. J., Farr, A. L., and Randall, R. J. (1951) Protein measurements with the Folin phenol reagent, *J. Biol. Chem. 193*, 265−275.
39. Birmachu, W., Nisswandt, F. L., and Thomas, D. D. (1989) Conformational transitions in the calcium adenosinetriphosphatase studied by time-resolved fluorescence resonance energy transfer, *Biochemistry 28*, 3940−7.
40. Reddy, L. G., Autry, J. M., Jones, L. R., and Thomas, D. D. (1999) Co-reconstitution of phospholamban mutants with the Ca-ATPase

reveals dependence of inhibitory function on phospholamban structure, *J. Biol. Chem. 274*, 7649−55.
41. Reddy, L. G., Jones, L. R., Cala, S. E., O'Brian, J. J., Tatulian, S. A., and Stokes, D. L. (1995) Functional reconstitution of recombinant phospholamban with rabbit skeletal Ca(2+)-ATPase, *J. Biol. Chem. 270*, 9390−7.
42. Reddy, L. G., Jones, L. R., Pace, R. C., and Stokes, D. L. (1996) Purified, reconstituted cardiac Ca^{2+}-ATPase is regulated by phospholamban but not by direct phosphorylation with Ca^{2+}/calmodulin- dependent protein kinase, *J. Biol. Chem. 271*, 14964−70.
43. Reddy, L. G., Cornea, R. L., Winters, D. L., McKenna, E., and Thomas, D. D. (2003) Defining the molecular components of calcium transport regulation in a reconstituted membrane system, *Biochemistry 42*, 4585−92.
44. Fabiato, A., and Fabiato, F. (1979) Calculator programs for computing the composition of the solutions containing multiple metals and ligands used for experiments in skinned muscle cells, *J. Physiol. (Paris) 75*, 463−505.
45. Li, M., Reddy, L. G., Bennett, R., Silva, N. D., Jr., Jones, L. R., and Thomas, D. D. (1999) A fluorescence energy transfer method for analyzing protein oligomeric structure: application to phospholamban, *Biophys. J. 76*, 2587−99.
46. Young, H. S., Jones, L. R., and Stokes, D. L. (2001) Locating phospholamban in co-crystals with Ca(2+)-ATPase by cryoelectron microscopy, *Biophys. J. 81*, 884−94.
47. Hutter, M. C., Krebs, J., Meiler, J., Griesinger, C., Carafoli, E., and Helms, V. (2002) A structural model of the complex formed by phospholamban and the calcium pump of sarcoplasmic reticulum obtained by molecular mechanics, *Chembiochem 3*, 1200−8.
48. Toyoshima, C., Asahi, M., Sugita, Y., Khanna, R., Tsuda, T., and MacLennan, D. H. (2003) Modeling of the inhibitory interaction of phospholamban with the Ca^{2+} ATPase, *Proc. Natl. Acad. Sci. U.S.A. 100*, 467−72.
49. Fung, B. K., and Stryer, L. (1978) Surface density determination in membranes by fluorescence energy transfer, *Biochemistry 17*, 5241−8.
50. Dewey, T. G., and Hammes, G. G. (1980) Calculation on fluorescence resonance energy transfer on surfaces, *Biophys. J. 32*, 1023−35.
51. Birmachu, W., and Thomas, D. D. (1990) Rotational dynamics of the Ca-ATPase in sarcoplasmic reticulum studied by time-resolved phosphorescence anisotropy, *Biochemistry 29*, 3904−14.
52. Laemmli, U. K. (1970) Cleavage of structural proteins during the assembly of the head of bacteriophage T4, *Nature 227*, 680−5.
53. Young, H. S., Rigaud, J. L., Lacapere, J. J., Reddy, L. G., and Stokes, D. L. (1997) How to make tubular crystals by reconstitution of detergent-solubilized Ca2(+)-ATPase, *Biophys. J. 72*, 2545−58.
54. Toyoshima, C., and Nomura, H. (2002) Structural changes in the calcium pump accompanying the dissociation of calcium, *Nature 418*, 605−11.
55. Toyoshima, C., Nakasako, M., Nomura, H., and Ogawa, H. (2000) Crystal structure of the calcium pump of sarcoplasmic reticulum at 2.6 A resolution, *Nature 405*, 647−55.
56. Ferrington, D. A., Yao, Q., Squier, T. C., and Bigelow, D. J. (2002) Comparable levels of Ca-ATPase inhibition by phospholamban in slow- twitch skeletal and cardiac sarcoplasmic reticulum, *Biochemistry 41*, 13289−96.
57. Briggs, F. N., Lee, K. F., Wechsler, A. W., and Jones, L. R. (1992) Phospholamban expressed in slow-twitch and chronically stimulated fast-twitch muscles minimally affects calcium affinity of sarcoplasmic reticulum Ca(2+)-ATPase, *J. Biol. Chem. 267*, 26056−61.
58. Colyer, J., and Wang, J. H. (1991) Dependence of cardiac sarcoplasmic reticulum calcium pump activity on the phosphorylation status of phospholamban, *J. Biol. Chem. 266*, 17486−93.
59. Negash, S., Chen, L. T., Bigelow, D. J., and Squier, T. C. (1996) Phosphorylation of phospholamban by cAMP-dependent protein kinase enhances interactions between Ca-ATPase polypeptide chains in cardiac sarcoplasmic reticulum membranes, *Biochemistry 35*, 11247−59.
60. Reddy, L. G., Jones, L. R., and Thomas, D. D. (1999) Depolymerization of phospholamban in the presence of calcium pump: a fluorescence energy transfer study, *Biochemistry 38*, 3954−62.
61. Mahaney, J. E., Froechlich, J. P., and Thomas, D. D. (1995) Conformational transitions of the sarcoplasmic reticulum Ca-ATPase studied by time-resolved EPR and quenched-flow kinetics, *Biochemistry 34*, 4864−79.
62. Kirby, T. L., Karim, C. B., and Thomas, D. D. (2004) EPR reveals a large-scale conformational change in the cytoplasmic domain of PLB upon binding to the SR Ca-ATPase, *Biochemistry 42*, 5842−52.
63. Karon, B. S., Autry, J. M., Shi, Y., Garnett, C. E., Inesi, G., Jones, L. R., Kutchai, H., and Thomas, D. D. (1999) Different anesthetic sensitivities of skeletal and cardiac isoforms of the Ca-ATPase, *Biochemistry 38*, 9301−7.
64. Xu, C., Rice, W. J., He, W., and Stokes, D. L. (2002) A structural model for the catalytic cycle of Ca(2+)-ATPase, *J. Mol. Biol. 316*, 201−11.
65. Birmachu, W., Voss, J. C., Louis, C. F., and Thomas, D. D. (1993) Protein and lipid rotational dynamics in cardiac and skeletal sarcoplasmic reticulum detected by EPR and phosphorescence anisotropy, *Biochemistry 32*, 9445−53.
66. Kutchai, H., Mahaney, J. E., Geddis, L. M., and Thomas, D. D. (1994) Hexanol and lidocaine affect the oligomeric state of the Ca-ATPase of sarcoplasmic reticulum, *Biochemistry 33*, 13208−22.
67. Voss, J. C., Mahaney, J. E., and Thomas, D. D. (1995) Mechanism of Ca-ATPase inhibition by melittin in skeletal sarcoplasmic reticulum, *Biochemistry 34*, 930−9.
68. Karon, B. S., Mahaney, J. E., and Thomas, D. D. (1994) Halothane and cyclopiazonic acid modulate Ca-ATPase oligomeric state and function in sarcoplasmic reticulum, *Biochemistry 33*, 13928−37.

BI049732K